Published in final edited form as:

Semin Musculoskelet Radiol. 2017 September ; 21(4): 459–469. doi:10.1055/s-0037-1604007.

Advanced MRI Techniques for Muscle Imaging

Vivek Kalia, MD, MPH, MS[1], **Doris G. Leung, MD, PhD**[2], **Darryl B. Sneag, MD**[1], **Filippo Del Grande, MD, MBA**[3], and **John A. Carrino, MD, MPH**[1]

[1]Department of Radiology and Imaging, Hospital for Special Surgery, New York, New York [2]The Center for Genetic Muscle Disorders, Kennedy Krieger Institute, Baltimore, Maryland [3]Servizio si Radiologia del Sottoceneri, Ospedale Regionale di Lugano, Lugano, Ticino, Switzerland

Abstract

Advanced magnetic resonance imaging (MRI) techniques can evaluate a wide array of muscle pathologies including acute or chronic muscle injury, musculotendinous response to injury, intramuscular collections and soft tissue masses, and others. In recent years, MRI has played a more important role in muscle disease diagnosis and monitoring. MRI provides excellent spatial and contrast resolution and helps direct optimal sites for muscle biopsy. Whole-body MRI now helps identify signature patterns of muscular involvement in large anatomical regions with relative ease. Quantitative MRI has advanced the evaluation and disease tracking of muscle atrophy and fatty infiltration in entities such as muscular dystrophies. Multivoxel magnetic resonance spectroscopy (MRS) now allows a more thorough, complete evaluation of a muscle of interest without the inherent sampling bias of single-voxel MRS or biopsy. Diffusion MRI allows quantification of muscle inflammation and capillary perfusion as well as muscle fiber tracking.

Keywords

MRI; muscle; quantitative MRI; MR spectroscopy; diffusion imaging

Advanced magnetic resonance imaging (MRI) techniques can evaluate a wide array of muscle pathologies including acute or chronic muscle injury, degree of musculotendinous response to injury (e.g., scar formation, stiffness), intramuscular collections and soft tissue masses, and others.

Most advanced MRI techniques available to date are not used routinely for the clinical evaluation of muscle. However, in some clinical areas such as neuromuscular diseases, MRI is becoming more commonplace for disease diagnosis and monitoring. MRI provides excellent spatial and contrast resolution for the evaluation of individual muscles, tendons,

Address for correspondence Vivek Kalia, MD, MPH, MS, Musculoskeletal Radiology Fellow, Hospital for Special Surgery, 535 E. 70th Street, PGY-6, New York, NY 10021 (vivekkalia@gmail.com).

Conflict of Interest

John A. Carrino is a consultant for General Electric, Pfizer, and Globus Medical. Darryl B. Sneag reports the following disclosure: Hospital for Special Surgery has an institutional research agreement with GE Healthcare. The remaining authors have nothing to disclose. The radiology department in Lugano has an institutional agreement as a reference center and for research projects with Siemens. Dr. Del Grande received a speaking honorarium from Bayer.

and musculotendinous units, as well as of large muscle groups for determining disease extent. MRI may also help direct optimal sites for muscle biopsy in regions of abnormal muscle signal intensity, volume, shape, or composition.[1, 2] Macroscopic structural changes in muscle, such as muscle atrophy and fatty infiltration[3–5] (►Fig. 1), occur after a cascade of more subtle microscopic changes takes hold. Such microscopic changes may include expansion of the extracellular volume (presenting as muscular edema), changes in muscle fiber shape, muscular necrosis, inflammation of muscle fibers (myositis), or fatty infiltration of muscle tissue.[6] Advances in MRI that can detect these pathologic events are critical for earlier diagnosis and earlier treatment of muscle disease.

High Field Strength

High field strength magnets more easily support higher spatial resolution for improved characterization of muscle injuries that most often occur around the myotendinous junction.[7] Such injuries may include areas of hemorrhage or interstitial edema that are best appreciated on fluid-sensitive sequences and have a classic feathery appearance.

Higher field strength magnets also allow for better characterization of muscle injuries in sports, for which a new categorization scheme was published in 2013 in the Munich consensus statement.[8] As healing occurs after muscle injury, there is resolution of the high signal intensity seen on fluid-sensitive sequences and often concomitant development of fibrous scarring that may initially be seen as high signal intensity on fluid-sensitive sequences but is eventually low signal intensity on all sequences. Because of differences in tear patterns and healing patterns, tears of even the same tendon at similar sites seen in different patients may yield different long-term functional outcomes because the mechanics of contraction during activity and risk of retear change.[9] The clinical relevance of the presence of scar and residual high signal within previously injured musculotendinous units remains uncertain.[10]

Whole-Body MRI

The size of the anatomical region that could be scanned in one encounter was traditionally limited by the time needed for image acquisition. In general, there is a trade-off between field of view and spatial resolution. Thus, whole-body MRI is more focused on the contrast resolution, provided by fluid/fat-sensitive sequences, rather than architectural detail. In cases where multiple anatomical regions needed to be scanned, individual regions were scanned one station at a time (often requiring patient repositioning between each scan) and later combined in the postprocessing phase. Advances in MR technique and technology, such as parallel acquisition techniques and continuous table movement, have allowed significant reductions in acquisition time while maintaining the image quality of whole-body MRI scans.[11]

One of the fields that was among the earliest to explore the clinical applications of whole-body MRI was oncology because metastatic disease can occur in multiple widely distributed organ systems.[12] Whole-body MRI can also be used to evaluate pathology that affects large portions of a patient’s muscular anatomy simultaneously, as is seen in many pediatric[13] and

adult myopathies, inherited muscle disorders such as Duchenne's muscular dystrophy (DMD),[14] and delayed-onset muscle soreness (DOMS). Heat maps that visually depict fatty infiltration scores of muscles throughout the body can then be constructed to display a group of patients' overall burden of muscle fatty infiltration (►Fig. 2).

MRI in general, and whole-body MRI in particular, can also serve as a useful adjunct to muscle biopsy and/or genetic analysis in the evaluation of pediatric myopathies.[1, 2, 15] Some key features assessed with whole-body MRI that might otherwise be missed on more limited scans including the distribution of proximal versus distal abnormalities (within a limb or within an individual muscle); preferential sparing or involvement of individual muscles or muscle groups across different body regions; the type of involvement of specific muscles (e.g., perifascial high signal intensity, atrophy) at various stages of disease; differences in the expected versus observed muscle bulk (atrophy versus hypertrophy) in individual muscles; and changes in total muscle mass.[13, 16]

A field of view that encompasses the entire body can further assist in evaluation of unilateral findings by allowing a comparison with the unaffected contralateral side. Whole-body MRI protocols most frequently include T1-weighted, T2-weighted, and short tau inversion recovery (STIR) sequences in the coronal and axial planes (►Fig. 3). Whole-body MRI using these sequences can be used to identify signature patterns of muscular involvement in disorders such as facioscapulohumeral muscular dystrophy (FSHD).[17] Ongoing research has begun to incorporate more diverse imaging sequences, such as diffusion-weighted imaging,[18] contrast-enhanced imaging,[19] and positron emission tomography,[20] into whole-body MR imaging protocols.

Quantitative MRI

Quantitative MRI, in which measurements such as fat quantification within muscle can be made, has become an increasingly important tool for the initial diagnosis of muscular disorders, disease tracking, and for evaluation of treatment efficacy. For example, investigators published the main findings in the various types of limb girdle muscle dystrophies in 2015 that provide a useful atlas both for initial clinical diagnosis and for disease tracking.[21]

Other investigators have used approaches based on chemical shift such as Dixon MRI to quantitate the long-term sequelae of denervation, such as muscular atrophy, fatty infiltration, and interstitial fibrosis, all of which may occur in traumatic brachial plexus injury.[22] This technique attempts to improve on the prior qualitative strategies of estimating muscle degeneration, such as the Goutallier score on T1-weighted turbo spin-echo images[23] that is moderately reliable at best even in experienced hands.[24] Another semiquantitative method called Mercuri scoring evaluates fibrofatty replacement of muscle by scoring on T1-weighted images.[25, 26]

In recent years, several groups have shown that a more robust quantitative measurement strategy is more sensitive in detecting small changes in muscle degeneration compared with a more qualitative method that focuses, for instance, on total muscle cross-sectional area and

a subjective assessment of fatty infiltration.[27, 28] Quantitative muscle MRI indeed detects subclinical muscular disease progression and can be used as a powerful surrogate outcome measure in clinical trials, although not yet approved by the U.S. Food and Drug Administration or the European Medicines Agency for this purpose.[29]

Dixon sequences (►Fig. 4) have shown utility in measuring intramuscular fat in patients with rotator cuff tears,[30, 31] muscular dystrophies,[32–38] and diabetes mellitus.[39] Quantitative Dixon techniques, provide the additional advantage of separating the portions of muscle within a cross section that consist of contractile muscle tissue from those that contain fatinfiltrated tissue. In so doing, it can provide a more accurate estimate of functional muscle bulk that may explain patients' symptoms better than simplyan overall cross-sectional area.[22] Three-point Dixon has been shown to quantify intramuscular fat and total and contractile cross-sectional areas with excellent interobserver reliability in brachial plexus injury patients.[22] Furthermore, these investigators quantitatively showed that in the studied patient cohort, the contractile cross-sectional area of the affected biceps brachii muscle contributed most to reduction in active elbow flexion, active supination, and muscle force. Qualitative, T2-weighted Dixon fat suppression techniques may also improve conspicuity of subtle muscle edema pattern in early denervation stages, as compared with conventional STIR or chemical fat suppression sequences (►Fig. 5). IDEAL is a three-echo Dixon technique for fat and water separation with a focus on noise performance and can be used with gradient-echo–based and spin-echo–based methods.

Three-dimensional MRI sequences may be used to assess overall muscle bulk in patients with muscle-wasting conditions or after trauma, such as after anterior cruciate ligament (ACL) injury[40–42] and reconstruction.[43–47] Such techniques have been used to show, for instance, that the ipsilateral gracilis and semitendinosus muscles in patients undergoing ACL reconstruction with hamstring tendon autograft experienced the highest degree of volumetric decline from pre- to postsurgery, likely due to selective atrophy from graft harvesting.[48]

Magnetic Resonance Spectroscopy

Magnetic resonance spectroscopy (MRS) provides information about the composition of tissues by separating metabolites according to their unique chemical shift properties. Since the 1980s, multiple investigators have used MRS to study phosphorus-containing (31P) compounds in muscle.[49] Because 31P is a component of adenosine triphosphate, phosphocreatine, and inorganic phosphate, 31P-MRS has been used to study patterns of energy consumption and exercise-related changes in muscle.[50, 51] Animal and human studies have identified metabolic profiles on 31P spectroscopy that correspond to muscle degeneration and regeneration in DMD, and similar findings have been reported in FSHD.[52–54] Furthermore, investigators have shown that 31P-containing metabolite concentrations measured using MRS correspond to the extent and rate of fat replacement in specific muscles as well as muscle strength in FSHD.[55]

In spite of the demonstrated utility of 31P-based MRS in studies of skeletal muscle, the need for specialized hardware, software, and expertise has limited its clinical applicability. More recent investigations in skeletal muscle have focused on the development of proton (1H)-

MRS that does not require additional hardware or software for most MR scanning systems.[56–58] One of the technical challenges in performing 1H-MRS in muscle has been the presence of large water and fat peaks that obscure smaller peaks corresponding to molecules of interest. Improvements in magnetic field homogeneity, gradients, and water suppression have now made it possible to use proton spectroscopy to estimate reliably the concentration of metabolites such as creatine and trimethylamines in muscle.[59] 1H-MRS can also be used to distinguish the intramuscular and extramuscular lipid peaks within muscle, allowing for noninvasive measurement of fatty infiltration.[60, 61] In muscle, 1H-MRS is now considered a reference standard for noninvasive quantification of fat.[62, 63] Because fat infiltration is a prominent pathologic feature of the muscular dystrophies and other chronic muscle disorders, this capability may be useful in characterizing pathology in this group of diseases. However, an important assumption of MRS is that the water content within muscle is consistent throughout, which may not be the case in particular conditions where inflammation/edema may coexist with fatty infiltration, such as in DMD.[64, 65]

Another advancement in MRS technique that may enhance its ability to examine muscle tissue is the ability to image multiple voxels in a single acquisition. Routine single-voxel spectroscopy protocols share the same disadvantages as a routine muscle biopsy in that they examine small regions of large muscles and can therefore miss areas of disease pathology. Performing MRS in multiple voxels previously required a greater number of phase-encoding steps that increased the scan time prohibitively. However, the development of various fast MRS techniques (such as multiple-echo acquisition, echo-planar spectroscopy imaging, and parallel encoded MRS) has reduced the scan time and allowed the efficient acquisition of spectra over large regions. These spectra can then be mapped onto anatomical images (►Figs. 6 and 7) to better appreciate spatial variations in the metabolic profile over large regions of tissue.[66, 67]

Studies of 1H-MRS in skeletal muscle in patients with myositis have shown that creatine concentrations in muscles that appear normal on T1 and STIR images are higher in patients with myositis compared with healthy controls, suggesting that changes in MRS profiles may precede pathologic changes on anatomical MRI.[68] The discovery of alterations in metabolite concentrations that precede both fat infiltration and clinical symptoms in skeletal muscle is an important one because it could distinguish early disease-related changes that are potentially reversible.

Blood Oxygenation-Level Dependent and Arterial Spin Labeling Imaging

Blood oxygenation-level dependent (BOLD) imaging, more commonly seen and associated with neuroimaging in functional brain imaging studies, can be used in musculoskeletal imaging to identify skeletal muscles with extensive but transient alterations of blood flow between resting and active states.[69] BOLD MR imaging is believed to be a better tool to provide functional information about muscle tissues and affords the possibility of superimposing high-resolution anatomical images,[69] whereas arterial spin labeling is more limited by poor contrast-to-noise ratio, higher motion sensitivity, and only moderate spatial resolution.[70] Still, BOLD MRI for skeletal muscle remains of limited clinical utility in most centers because it requires provocation maneuvers to induce measurable BOLD signal

alterations in skeletal muscle, such as cuff compression–induced ischemia, exercise, administration of vasoactive pharmaceuticals, or oxygen ventilation.[71–73]

Furthermore, several known factors can affect BOLD signal in skeletal muscle including patient age, recent exercise activity, muscle fiber type, and certain vasoactive pharmaceuticals,[69] all of which may need to be accounted for when interpreting BOLD MR images that may add to interpretation time. Similar to 31P-based MRS in studies of skeletal muscle, the need for specialized software and clinical expertise in BOLD imaging has limited its clinical applicability.

T2 Mapping

T2 mapping is a quantitative MR technique that measures T2 relaxation times throughout the tissue of interest. Areas of increased free water (e.g., areas of inflammation) manifest as higher T2 values; indeed, nearly all pathophysiologic states of muscle increase T2 relaxation times.[74] T2 mapping may also be used to track changes in muscle after therapy, for example after botulinum toxin injection into the gastrocnemius muscle (►Fig. 8).[75] T2 mapping allows for evaluation of muscle activity, with proportionally higher T2 values seen with higher activity in involved muscles.[76, 77] T2 mapping can also be used to evaluate muscle inflammation[78] and fatty infiltration.[79] An important technical consideration when performing T2 mapping is to construct T2 maps with fat suppression, so the measured T2 relaxation times reflect only increased T2 values due to edema (and not due to fatty infiltration of the muscles that will artifactually elevate T2 values on non–fat-suppressed T2 maps).[74, 80] That small amounts of intramuscular fat could be quantified using T2 mapping with and without fat suppression was validated by Shiraj et al in 2014.[81] In addition to the quantitative aspects of T2 mapping, it can also improve the conspicuity of and confirm subtle abnormalities such as early denervation (►Fig. 9).

Diffusion MRI

Muscle is an ordered fibrillar biological tissue that exhibits tissue anisotropy (i.e., diffusion of water is not unrestricted in all directions).[82–86] Muscular diffusion values also depend on the orientation of muscle fibers because the motion of water is least restricted parallel to fibers. Diffusion-weighted imaging (DWI) offers the opportunity to measure molecular diffusion noninvasively and to make meaningful inferences from such information in clinical contexts.[87] In inflamed muscles, diffusion may be increased because of fluid infiltrating the extracellular space. However, in the idiopathic inflammatory myopathies, small capillary diffusion volumes indicate a reduced vascular supply. DWI is able to quantify muscle inflammation and capillary perfusion with the ability to monitor the integrity of the myofibrillar lattice in myositis.[88]

Diffusion Tensor Imaging

Diffusion tensor imaging (DTI) allows for quantification of diffusion in muscle and for muscle fiber tracking (e.g., to track skeletal muscle fiber direction and subclinical injury in skeletal muscles on a microscopic level).[89–91] Damage to muscle resulting from ischemic,

inflammatory, and traumatic processes may result in muscle fiber disorganization and deterioration that can be indirectly measured with diffusion tensor parameters such as mean diffusivity and fractional anisotropy (FA).[87, 92] Indeed, multiple prior studies have shown that muscle filament size and cross-sectional area of a bulk muscle do not directly depend on each other,[6, 93–95] and they suggest that more microscopic changes must be evaluated, such as with diffusion MRI. Prior studies showed little diffusion restriction along muscle fibers and strong restriction transverse to muscle fibers, supported by a study using time-dependent DTI.[96] Other groups have found DTI to serve as a promising ancillary imaging method (to standard T2 weighted imaging) in the diagnosis of chronic exertional compartment syndrome of the lower extremities[97] (►Fig. 10), in which the muscular compartments retain excess fluid following exercise, potentially leading to perfusion abnormalities, pain, and ischemic muscle injury.[98] FA maps may be reconstructed from diffusion images and used in muscle imaging. In one recent study, FA maps were shown to have a very strong inverse correlation (Pearson correlation coefficient [R] = − 0.993, with $p = 0.001$) with pain in the context of DOMS and have been proposed to better reflect underlying muscle damage because intramuscular and perifascial edema may persist long after the resolution of clinical symptoms, whereas FA normalizes around the same time as pain subsides.[99]

Magnetic Resonance Elastography

Magnetic resonance elastography (MRE) infers the mechanical properties (e.g., stiffness) of soft tissues by analyzing shear wave data. MRE may be used to evaluate for differences in physiologic responses and stiffness between normal and damaged muscles.[100, 101] For instance, after 48 hours following an eccentric exercise protocol, an increase in the magnitude of muscle shear stiffness may be seen in postexercise muscles compared with the same muscles before exercise.[7]

Acknowledgments

The authors would like to acknowledge contributions from Eric E. Sigmund, PhD (NYU Langone Medical Center), Jonathan P. Dyke, PhD (Weill Cornell Medicine), and Michael O'Dell, MD (Weill Cornell Medicine).

Funding Source

Doris G. Leung receives support from a National Institutes of Health grant (5 K23 NS091379–03).

References

1. Mercuri E, Jungbluth H, Muntoni F. Muscle imaging in clinical practice: diagnostic value of muscle magnetic resonance imaging in inherited neuromuscular disorders. Curr Opin Neurol. 2005; 18(05): 526–537. [PubMed: 16155435]
2. Mercuri E, Pichiecchio A, Allsop J, Messina S, Pane M, Muntoni F. Muscle MRI in inherited neuromuscular disorders: past, present, and future. J Magn Reson Imaging. 2007; 25(02):433–440. [PubMed: 17260395]
3. Barry JJ, Lansdown DA, Cheung S, Feeley BT, Ma CB. The relationship between tear severity, fatty infiltration, and muscle atrophy in the supraspinatus. J Shoulder Elbow Surg. 2013; 22(01):18–25. [PubMed: 22541866]
4. Meyer DC, Hoppeler H, von Rechenberg B, Gerber C. A pathomechanical concept explains muscle loss and fatty muscular changes following surgical tendon release. J Orthop Res. 2004; 22(05): 1004–1007. [PubMed: 15304272]

5. Matsumoto F, Uhthoff HK, Trudel G, Loehr JF. Delayed tendon reattachment does not reverse atrophy and fat accumulation of the supraspinatus—an experimental study in rabbits. J Orthop Res. 2002; 20(02):357–363. [PubMed: 11918317]
6. Fieremans E, Lemberskiy G, Veraart J, Sigmund EE, Gyftopoulos S, Novikov DS. In vivo measurement of membrane permeability and myofiber size in human muscle using time-dependent diffusion tensor imaging and the random permeable barrier model. NMR Biomed. 2017; 30(03)
7. Guermazi A, Roemer FW, Robinson P, Tol JL, Regatte RR, Crema MD. Imaging of muscle injuries in sports medicine: sports imaging series. Radiology. 2017; 282(03):646–663. [PubMed: 28218878]
8. Mueller-Wohlfahrt HW, Haensel L, Mithoefer K, et al. Terminology and classification of muscle injuries in sport: the Munich consensus statement. Br J Sports Med. 2013; 47(06):342–350. [PubMed: 23080315]
9. Silder A, Heiderscheit BC, Thelen DG, Enright T, Tuite MJ. MR observations of long-term musculotendon remodeling following a hamstring strain injury. Skeletal Radiol. 2008; 37(12):1101–1109. [PubMed: 18649077]
10. Reurink G, Goudswaard GJ, Tol JL, et al. MRI observations at return to play of clinically recovered hamstring injuries. Br J Sports Med. 2014; 48(18):1370–1376. [PubMed: 24255767]
11. Weckbach S, Michaely HJ, Stemmer A, Schoenberg SO, Dinter DJ. Comparison of a new whole-body continuous-table-movement protocol versus a standard whole-body MR protocol for the assessment of multiple myeloma. Eur Radiol. 2010; 20(12):2907–2916. [PubMed: 20574630]
12. Guimarães MD, Noschang J, Teixeira SR, et al. Whole-body MRI in pediatric patients with cancer. Cancer Imaging. 2017; 17(01):6. [PubMed: 28187778]
13. Cejas CP, Serra MM, Galvez DFG, et al. Muscle MRI in pediatrics: clinical, pathological and genetic correlation. Pediatr Radiol. 2017; 47(06):724–735. [PubMed: 28102454]
14. Polavarapu K, Manjunath M, Preethish-Kumar V, et al. Muscle MRI in Duchenne muscular dystrophy: evidence of a distinctive pattern. Neuromuscul Disord. 2016; 26(11):768–774. [PubMed: 27666775]
15. Bönnemann CG, Wang CH, Quijano-Roy S, et al. Members of International Standard of Care Committee for Congenital Muscular Dystrophies. Diagnostic approach to the congenital muscular dystrophies. Neuromuscul Disord. 2014; 24(04):289–311. [PubMed: 24581957]
16. Schmidt GP, Reiser MF, Baur-Melnyk A. Whole-body imaging of the musculoskeletal system: the value of MR imaging. Skeletal Radiol. 2007; 36(12):1109–1119. [PubMed: 17554538]
17. Leung DG, Carrino JA, Wagner KR, Jacobs MA. Whole-body magnetic resonance imaging evaluation of facioscapulohumeral muscular dystrophy. Muscle Nerve. 2015; 52(04):512–520. [PubMed: 25641525]
18. Perez-Lopez R, Mateo J, Mossop H, et al. Diffusion-weighted imaging as a treatment response biomarker for evaluating bone metastases in prostate cancer: a pilot study. Radiology. 2017; 283(01):168–177. [PubMed: 27875103]
19. Kono M, Kamishima T, Yasuda S, et al. Effectiveness of whole-body magnetic resonance imaging for the efficacy of biologic anti-rheumatic drugs in patients with rheumatoid arthritis: A retrospective pilot study. Mod Rheumatol. 2017 Feb 1. (Epub ahead of print).
20. Sawicki LM, Grueneisen J, Buchbender C, et al. Comparative performance of ^{18}F-FDG PET/MRI and ^{18}F-FDG PET/CT in detection and characterization of pulmonary lesions in 121 oncologic patients. J Nucl Med. 2016; 57(04):582–586. [PubMed: 26742715]
21. Díaz-Manera J, Llauger J, Gallardo E, Illa I. Muscle MRI in muscular dystrophies. Acta Myol. 2015; 34(2–3):95–108. [PubMed: 27199536]
22. Duijnisveld BJ, Henseler JF, Reijnierse M, Fiocco M, Kan HE, Nelissen RG. Quantitative Dixon MRI sequences to relate muscle atrophy and fatty degeneration with range of motion and muscle force in brachial plexus injury. Magn Reson Imaging. 2017; 36:98–104. [PubMed: 27989913]
23. Hogendoorn S, van Overvest KL, Watt I, Duijsens AH, Nelissen RG. Structural changes in muscle and glenohumeral joint deformity in neonatal brachial plexus palsy. J Bone Joint Surg Am. 2010; 92(04):935–942. [PubMed: 20360518]
24. Slabaugh MA, Friel NA, Karas V, Romeo AA, Verma NN, Cole BJ. Interobserver and intraobserver reliability of the Goutallier classification using magnetic resonance imaging:

proposal of a simplified classification system to increase reliability. Am J Sports Med. 2012; 40(08):1728–1734. [PubMed: 22753846]

25. Mercuri E, Talim B, Moghadaszadeh B, et al. Clinical and imaging findings in six cases of congenital muscular dystrophy with rigid spine syndrome linked to chromosome 1p (RSMD1). Neuromuscul Disord. 2002; 12(7–8):631–638. [PubMed: 12207930]
26. Borsato C, Padoan R, Stramare R, Angelini C. Limb-girdle muscular dystrophies type 2A and 2B: clinical and radiological aspects. Basic Appl Myol. 2006; 16:17–25.
27. Fischmann A, Hafner P, Fasler S, et al. Quantitative MRI can detect subclinical disease progression in muscular dystrophy. J Neurol. 2012; 259(08):1648–1654. [PubMed: 22297459]
28. Willis TA, Hollingsworth KG, Coombs A, et al. Quantitative magnetic resonance imaging in limb-girdle muscular dystrophy 2I: a multinational cross-sectional study. PLoS One. 2014; 9(02):e90377. [PubMed: 24587344]
29. Fischer D, Bonati U, Wattjes MP. Recent developments in muscle imaging of neuromuscular disorders. Curr Opin Neurol. 2016; 29(05):614–620. [PubMed: 27427989]
30. Lee S, Lucas RM, Lansdown DA, et al. Magnetic resonance rotator cuff fat fraction and its relationship with tendon tear severityand subject characteristics. J Shoulder Elbow Surg. 2015; 24(09):1442–1451. [PubMed: 25819731]
31. Nardo L, Karampinos DC, Lansdown DA, et al. Quantitative assessment of fat infiltration in the rotator cuff muscles using water-fat MRI. J Magn Reson Imaging. 2014; 39(05):1178–1185. [PubMed: 24115490]
32. Wren TA, Bluml S, Tseng-Ong L, Gilsanz V. Three-point technique of fat quantification of muscle tissue as a marker of disease progression in Duchenne muscular dystrophy: preliminary study. AJR Am J Roentgenol. 2008; 190(01):W8–12. [PubMed: 18094282]
33. Wokke BH, Bos C, Reijnierse M, et al. Comparison of Dixon and T1-weighted MR methods to assess the degree of fat infiltration in Duchenne muscular dystrophy patients. J Magn Reson Imaging. 2013; 38(03):619–624. [PubMed: 23292884]
34. van den Bergen JC, Wokke BH, Janson AA, et al. Dystrophin levels and clinical severity in Becker muscular dystrophy patients. J Neurol Neurosurg Psychiatry. 2014; 85(07):747–753. [PubMed: 24292997]
35. Triplett WT, Baligand C, Forbes SC, et al. Chemical shift-based MRI to measure fat fractions in dystrophic skeletal muscle. Magn Reson Med. 2014; 72(01):8–19. [PubMed: 24006208]
36. Paradas C, Llauger J, Diaz-Manera J, et al. Redefining dysferlinopathy phenotypes based on clinical findings and muscle imaging studies. Neurology. 2010; 75(04):316–323. [PubMed: 20574037]
37. Dahlqvist JR, Vissing CR, Thomsen C, Vissing J. Severe paraspinal muscle involvement in facioscapulohumeral muscular dystrophy. Neurology. 2014; 83(13):1178–1183. [PubMed: 25142899]
38. Tasca G, Iannaccone E, Monforte M, et al. Muscle MRI in Becker muscular dystrophy. Neuromuscul Disord. 2012; 22(Suppl 2):S100–S106. [PubMed: 22980760]
39. Karampinos DC, Baum T, Nardo L, et al. Characterization of the regional distribution of skeletal muscle adipose tissue in type 2 diabetes using chemical shift-based water/fat separation. J Magn Reson Imaging. 2012; 35(04):899–907. [PubMed: 22127958]
40. Williams GN, Buchanan TS, Barrance PJ, Axe MJ, Snyder-Mackler L. Quadriceps weakness, atrophy, and activation failure in predicted noncopers after anterior cruciate ligament injury. Am J Sports Med. 2005; 33(03):402–407. [PubMed: 15716256]
41. Macleod TD, Snyder-Mackler L, Buchanan TS. Differences in neuromuscular control and quadriceps morphology between potential copers and noncopers following anterior cruciate ligament injury. J Orthop Sports Phys Ther. 2014; 44(02):76–84. [PubMed: 24261930]
42. Williams GN, Snyder-Mackler L, Barrance PJ, Buchanan TS. Quadriceps femoris muscle morphology and function after ACL injury: a differential response in copers versus non-copers. J Biomech. 2005; 38(04):685–693. [PubMed: 15713288]
43. Marcon M, Ciritsis B, Laux C, et al. Quantitative and qualitative MR-imaging assessment of vastus medialis muscle volume loss in asymptomatic patients after anterior cruciate ligament reconstruction. J Magn Reson Imaging. 2015; 42(02):515–525. [PubMed: 25446958]

44. Marcon M, Ciritsis B, Laux C, et al. Cross-sectional area measurements versus volumetric assessment of the quadriceps femoris muscle in patients with anterior cruciate ligament reconstructions. Eur Radiol. 2015; 25(02):290–298. [PubMed: 25358592]
45. Nomura Y, Kuramochi R, Fukubayashi T. Evaluation of hamstring muscle strength and morphology after anterior cruciate ligament reconstruction. Scand J Med Sci Sports. 2015; 25(03): 301–307. [PubMed: 24646218]
46. Snow BJ, Wilcox JJ, Burks RT, Greis PE. Evaluation of muscle size and fatty infiltration with MRI nine to eleven years following hamstring harvest for ACL reconstruction. J Bone Joint Surg Am. 2012; 94(14):1274–1282. [PubMed: 22810397]
47. Konishi Y, Fukubayashi T. Relationship between muscle volume and muscle torque of the hamstrings after anterior cruciate ligament reconstruction. J Sci Med Sport. 2010; 13(01):101–105. [PubMed: 18964233]
48. Norte GE, Knaus KR, Kuenze C, et al. MRI-based assessment of lower extremity muscle volumes in patients before and after ACL reconstruction. J Sport Rehabil. 2017 Mar 14. (Epub ahead of print).
49. Edwards RH, Dawson MJ, Wilkie DR, Gordon RE, Shaw D. Clinical use of nuclear magnetic resonance in the investigation of myopathy. Lancet. 1982; 1(8274):725–731. [PubMed: 6122019]
50. Barbiroli B, Funicello R, Ferlini A, Montagna P, Zaniol P. Muscle energy metabolism in female DMD/BMD carriers: a 31P-MR spectroscopy study. Muscle Nerve. 1992; 15(03):344–348. [PubMed: 1557082]
51. Kemp GJ, Taylor DJ, Dunn JF, Frostick SP, Radda GK. Cellular energetics of dystrophic muscle. J Neurol Sci. 1993; 116(02):201–206. [PubMed: 8393092]
52. Banerjee B, Sharma U, Balasubramanian K, Kalaivani M, Kalra V, Jagannathan NR. Effect of creatine monohydrate in improving cellular energetics and muscle strength in ambulatory Duchenne muscular dystrophy patients: a randomized, placebo-controlled 31P MRS study. Magn Reson Imaging. 2010; 28(05):698–707. [PubMed: 20395096]
53. Kan HE, Klomp DW, Wohlgemuth M, et al. Only fat infiltrated muscles in resting lower leg of FSHD patients show disturbed energy metabolism. NMR Biomed. 2010; 23(06):563–568. [PubMed: 20175146]
54. Heier CR, Guerron AD, Korotcov A, et al. Non-invasive MRI and spectroscopy of mdx mice reveal temporal changes in dystrophic muscle imaging and in energy deficits. PLoS One. 2014; 9(11):e112477. [PubMed: 25390038]
55. Janssen BH, Voet NB, Nabuurs CI, et al. Distinct disease phases in muscles of facioscapulohumeral dystrophy patients identified by MR detected fat infiltration. PLoS One. 2014; 9(01):e85416. [PubMed: 24454861]
56. Hsieh TJ, Jaw TS, Chuang HY, Jong YJ, Liu GC, Li CW. Muscle metabolism in Duchenne muscular dystrophy assessed by in vivo proton magnetic resonance spectroscopy. J Comput Assist Tomogr. 2009; 33(01):150–154. [PubMed: 19188804]
57. Willcocks RJ, Forbes SC, Finanger EL, et al. P.13.5 Magnetic resonance imaging and spectroscopy detect changes with age, corticosteroid treatment, and functional progression in DMD. Neuromuscul Disord. 2013; 23(9–10):810.
58. Kim HK, Serai S, Lindquist D, et al. Quantitative skeletal muscle MRI: Part 2, MR spectroscopy and T2 relaxation time mapping-comparison between boys with Duchenne muscular dystrophy and healthy boys. AJR Am J Roentgenol. 2015; 205(02):W216–W223. [PubMed: 26204310]
59. Bongers H, Schick F, Skalej M, Jung WI, Stevens A. Localized in vivo 1H spectroscopy of human skeletal muscle: normal and pathologic findings. Magn Reson Imaging. 1992; 10(06):957–964. [PubMed: 1461093]
60. Boesch C, Décombaz J, Slotboom J, Kreis R. Observation of intramyocellular lipids by means of 1H magnetic resonance spectroscopy. Proc Nutr Soc. 1999; 58(04):841–850. [PubMed: 10817151]
61. Boesch C, Machann J, Vermathen P, Schick F. Role of proton MR for the study of muscle lipid metabolism. NMR Biomed. 2006; 19(07):968–988. [PubMed: 17075965]
62. Fischer MA, Nanz D, Shimakawa A, et al. Quantification of muscle fat in patients with low back pain: comparison of multi-echo MR imaging with single-voxel MR spectroscopy. Radiology. 2013; 266(02):555–563. [PubMed: 23143025]

63. Reeder SB, Cruite I, Hamilton G, Sirlin CB. Quantitative assessment of liver fat with magnetic resonance imaging and spectroscopy. J Magn Reson Imaging. 2011; 34(04):729–749. [PubMed: 21928307]
64. Marden FA, Connolly AM, Siegel MJ, Rubin DA. Compositional analysis of muscle in boys with Duchenne muscular dystrophy using MR imaging. Skeletal Radiol. 2005; 34(03):140–148. [PubMed: 15538561]
65. Forbes SC, Willcocks RJ, Triplett WT, et al. Magnetic resonance imaging and spectroscopy assessment of lower extremity skeletal muscles in boys with Duchenne muscular dystrophy: a multicenter cross sectional study. PLoS One. 2014; 9(09):e106435. [PubMed: 25203313]
66. Nelson SJ. Multivoxel magnetic resonance spectroscopy of brain tumors. Mol Cancer Ther. 2003; 2(05):497–507. [PubMed: 12748312]
67. Fayad LM, Barker PB, Jacobs MA, et al. Characterization of musculoskeletal lesions on 3-T proton MR spectroscopy. AJR Am J Roentgenol. 2007; 188(06):1513–1520. [PubMed: 17515370]
68. Subhawong TK, Wang X, Machado AJ, et al. 1H Magnetic resonance spectroscopy findings in idiopathic inflammatory myopathies at 3 T: feasibility and first results. Invest Radiol. 2013; 48(07):509–516. [PubMed: 23563194]
69. Jacobi B, Bongartz G, Partovi S, et al. Skeletal muscle BOLD MRI: from underlying physiological concepts to its usefulness in clinical conditions. J Magn Reson Imaging. 2012; 35(06):1253–1265. [PubMed: 22588992]
70. Carlier PG, Bertoldi D, Baligand C, Wary C, Fromes Y. Muscle blood flow and oxygenation measured by NMR imaging and spectroscopy. NMR Biomed. 2006; 19(07):954–967. [PubMed: 17075963]
71. Li D, Dhawale P, Rubin PJ, Haacke EM, Gropler RJ. Myocardial signal response to dipyridamole and dobutamine: demonstration of the BOLD effect using a double-echo gradient-echo sequence. Magn Reson Med. 1996; 36(01):16–20. [PubMed: 8795015]
72. Donahue KM, Van Kylen J, Guven S, et al. Simultaneous gradient-echo/spin-echo EPI of graded ischemia in human skeletal muscle. J Magn Reson Imaging. 1998; 8(05):1106–1113. [PubMed: 9786149]
73. Wigmore DM, Damon BM, Pober DM, Kent-Braun JA. MRI measures of perfusion-related changes in human skeletal muscle during progressive contractions. J Appl Physiol (1985). 2004; 97(06):2385–2394. [PubMed: 15298991]
74. Johnston JH, Kim HK, Merrow AC, et al. Quantitative skeletal muscle MRI: Part 1, Derived T2 fat map in differentiation between boys with Duchenne muscular dystrophy and healthy boys. AJR Am J Roentgenol. 2015; 205(02):W207–W215. [PubMed: 26204309]
75. O'Dell MW, Villanueva M, Creelman C, et al. Detection of botulinum toxin muscle effect in humans using magnetic resonance imaging: a qualitative case series. PM R. 2017; (17):30551–30558. pii:S1934-1482.
76. Shellock FG, Fleckenstein JL. Muscle physiology and pathophysiology: magnetic resonance imaging evaluation. Semin Muscu-loskelet Radiol. 2000; 4(04):459–479.
77. Kinugasa R, Kawakami Y, Fukunaga T. Mapping activation levels of skeletal muscle in healthy volunteers: an MRI study. J Magn Reson Imaging. 2006; 24(06):1420–1425. [PubMed: 17078087]
78. Maillard SM, Jones R, Owens C, et al. Quantitative assessment of MRI T2 relaxation time of thigh muscles in juvenile dermatomyositis. Rheumatology (Oxford). 2004; 43(05):603–608. [PubMed: 14983103]
79. Kim HK, Laor T, Horn PS, Racadio JM, Wong B, Dardzinski BJ. T2 mapping in Duchenne muscular dystrophy: distribution of disease activity and correlation with clinical assessments. Radiology. 2010; 255(03):899–908. [PubMed: 20501727]
80. Arpan I, Forbes SC, Lott DJ, et al. T_2 mapping provides multiple approaches for the characterization of muscle involvement in neuromuscular diseases: a cross-sectional study of lower leg muscles in 5–15-year-old boys with Duchenne muscular dystrophy. NMR Biomed. 2013; 26(03):320–328. [PubMed: 23044995]
81. Shiraj S, Kim HK, Anton C, Horn PS, Laor T. Spatial variation of T2 relaxation times of patellar cartilage and physeal patency: an in vivo study in children and young adults. AJR Am J Roentgenol. 2014; 202(03):W292–7. [PubMed: 24555628]

82. Damon BM, Ding Z, Anderson AW, Freyer AS, Gore JC. Validation of diffusion tensor MRI-based muscle fiber tracking. Magn Reson Med. 2002; 48(01):97–104. [PubMed: 12111936]
83. Galbán CJ, Maderwald S, Uffmann K, de Greiff A, Ladd ME. Diffusive sensitivity to muscle architecture: a magnetic resonance diffusion tensor imaging study of the human calf. Eur J Appl Physiol. 2004; 93(03):253–262. [PubMed: 15322853]
84. Sinha S, Hodgson JA, Finni T, Lai AM, Grinstead J, Edgerton VR. Muscle kinematics during isometric contraction: development of phase contrast and spin tag techniques to study healthy and atrophied muscles. J Magn Reson Imaging. 2004; 20(06):1008–1019. [PubMed: 15558560]
85. Steidle G, Schick F. Echoplanar diffusion tensor imaging of the lower leg musculature using eddy current nulled stimulated echo preparation. Magn Reson Med. 2006; 55(03):541–548. [PubMed: 16450364]
86. Baete SH, Cho GY, Sigmund EE. Dynamic diffusion-tensor measurements in muscle tissue using the single-line multiple-echo diffusion-tensor acquisition technique at 3T. NMR Biomed. 2015; 28(06):667–678. [PubMed: 25900166]
87. Novikov DS, Jensen JH, Helpern JA, Fieremans E. Revealing mesoscopic structural universality with diffusion. Proc Natl Acad Sci U S A. 2014; 111(14):5088–5093. [PubMed: 24706873]
88. Qi J, Olsen NJ, Price RR, Winston JA, Park JH. Diffusion-weighted imaging of inflammatory myopathies: polymyositis and dermatomyositis. J Magn Reson Imaging. 2008; 27(01):212–217. [PubMed: 18022843]
89. Zaraiskaya T, Kumbhare D, Noseworthy MD. Diffusion tensor imaging in evaluation of human skeletal muscle injury. J Magn Reson Imaging. 2006; 24(02):402–408. [PubMed: 16823776]
90. Cermak NM, Noseworthy MD, Bourgeois JM, Tarnopolsky MA, Gibala MJ. Diffusion tensor MRI to assess skeletal muscle disruption following eccentric exercise. Muscle Nerve. 2012; 46(01):42–50. [PubMed: 22644795]
91. Froeling M, Oudeman J, Strijkers GJ, et al. Muscle changes detected with diffusion-tensor imaging after long-distance running. Radiology. 2015; 274(02):548–562. [PubMed: 25279435]
92. Heemskerk AM, Drost MR, van Bochove GS, van Oosterhout MFM, Nicolay K, Strijkers GJ. DTI-based assessment of ischemia-reperfusion in mouse skeletal muscle. Magn Reson Med. 2006; 56(02):272–281. [PubMed: 16826605]
93. Lundberg TR, Fernandez-Gonzalo R, Gustafsson T, Tesch PA. Aerobic exercise does not compromise muscle hypertrophy response to short-term resistance training. J Appl Physiol (1985). 2013; 114(01):81–89. [PubMed: 23104700]
94. Harber MP, Konopka AR, Undem MK, et al. Aerobic exercise training induces skeletal muscle hypertrophy and age-dependent adaptations in myofiber function in young and older men. J Appl Physiol (1985). 2012; 113(09):1495–1504. [PubMed: 22984247]
95. Häkkinen K, Pakarinen A, Kraemer WJ, Häkkinen A, Valkeinen H, Alen M. Selective muscle hypertrophy, changes in EMG and force, and serum hormones during strength training in older women. J Appl Physiol (1985). 2001; 91(02):569–580. [PubMed: 11457767]
96. Kim S, Chi-Fishman G, Barnett AS, Pierpaoli C. Dependence on diffusion time of apparent diffusion tensor of ex vivo calf tongue and heart. Magn Reson Med. 2005; 54(06):1387–1396. [PubMed: 16265644]
97. Sigmund EE, Sui D, Ukpebor O, et al. Stimulated echo diffusion tensor imaging and SPAIR T2 - weighted imaging in chronic exertional compartment syndrome of the lower leg muscles. J Magn Reson Imaging. 2013; 38(05):1073–1082. [PubMed: 23440764]
98. Mohler LR, Styf JR, Pedowitz RA, Hargens AR, Gershuni DH. Intramuscular deoxygenation during exercise in patients who have chronic anterior compartment syndrome of the leg. J Bone Joint Surg Am. 1997; 79(06):844–849. [PubMed: 9199381]
99. Agten CA, Buck FM, Dyer L, Flück M, Pfirrmann CW, Rosskopf AB. Delayed-onset muscle soreness: temporal assessment with quantitative MRI and shear-wave ultrasound elastography. AJR Am J Roentgenol. 2017; 208(02):402–412. [PubMed: 27845853]
100. Papazoglou S, Rump J, Braun J, Sack I. Shear wave group velocity inversion in MR elastography of human skeletal muscle. Magn Reson Med. 2006; 56(03):489–497. [PubMed: 16894586]

101. Basford JR, Jenkyn TR, An KN, Ehman RL, Heers G, Kaufman KR. Evaluation of healthy and diseased muscle with magnetic resonance elastography. Arch Phys Med Rehabil. 2002; 83(11): 1530–1536. [PubMed: 12422320]

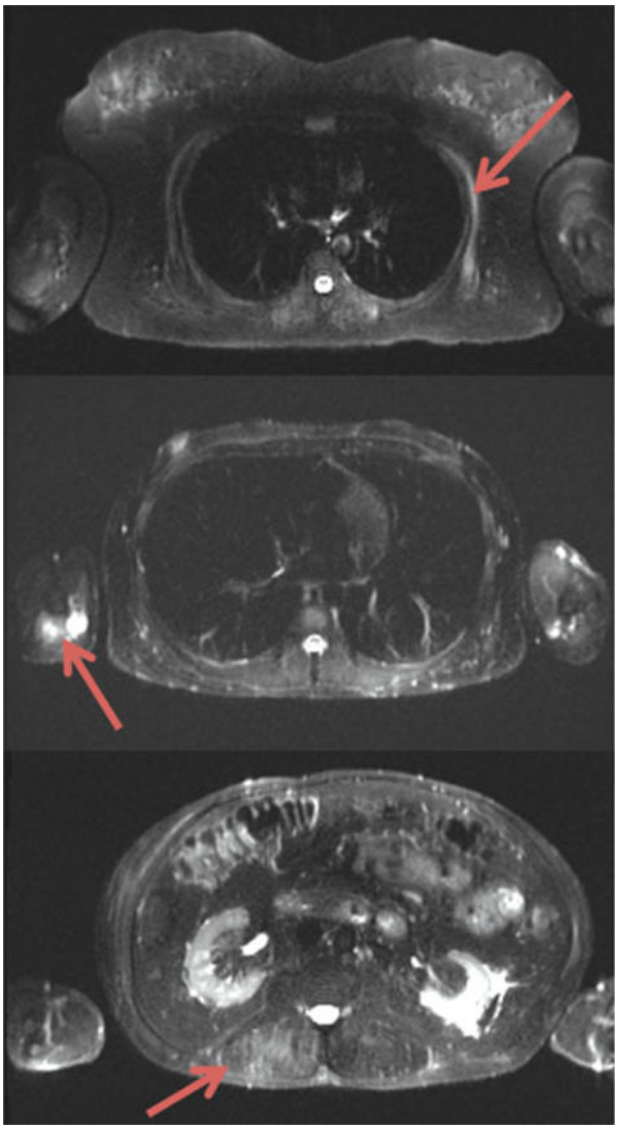

Fig. 1.

Axial short tau inversion recovery cross sections of the thorax and abdomen in a patient with facioscapulohumeral muscular dystrophy. Arrows denote active disease in the serratus anterior (upper image), triceps (middle image), and lumbar paraspinal muscles (lower image).

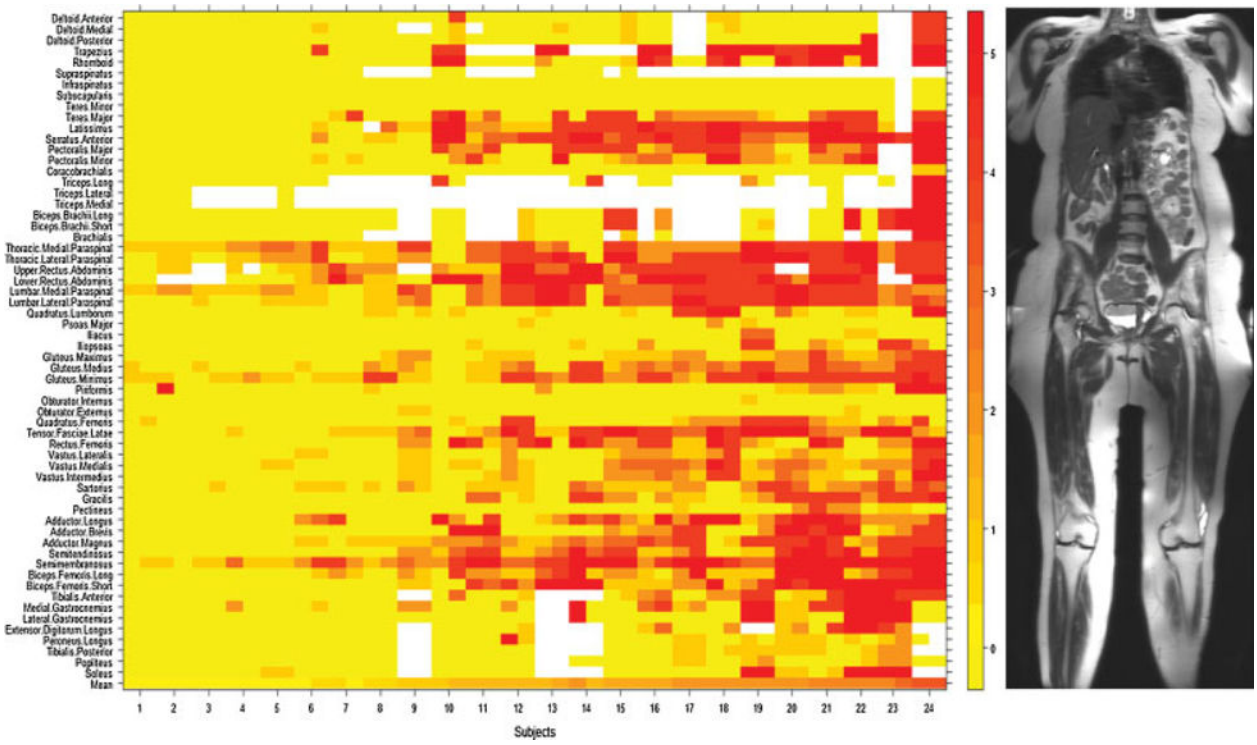

Fig. 2.

Heat map of fat infiltration scores in 24 individuals with facioscapulohumeral muscular dystrophy. Patients are arranged (left to right) from lowest to highest mean MRI score. Muscles on the left and right sides of the body are placed to the left and right sides (respectively) of the labeled tick marks for each subject. Fat infiltration scores on T1-weighted MRI (from 0 to 5) and their corresponding colors are shown in the numbered bar on the right. The mean MRI score for all muscles scored within a single individual are represented in the bottom row.

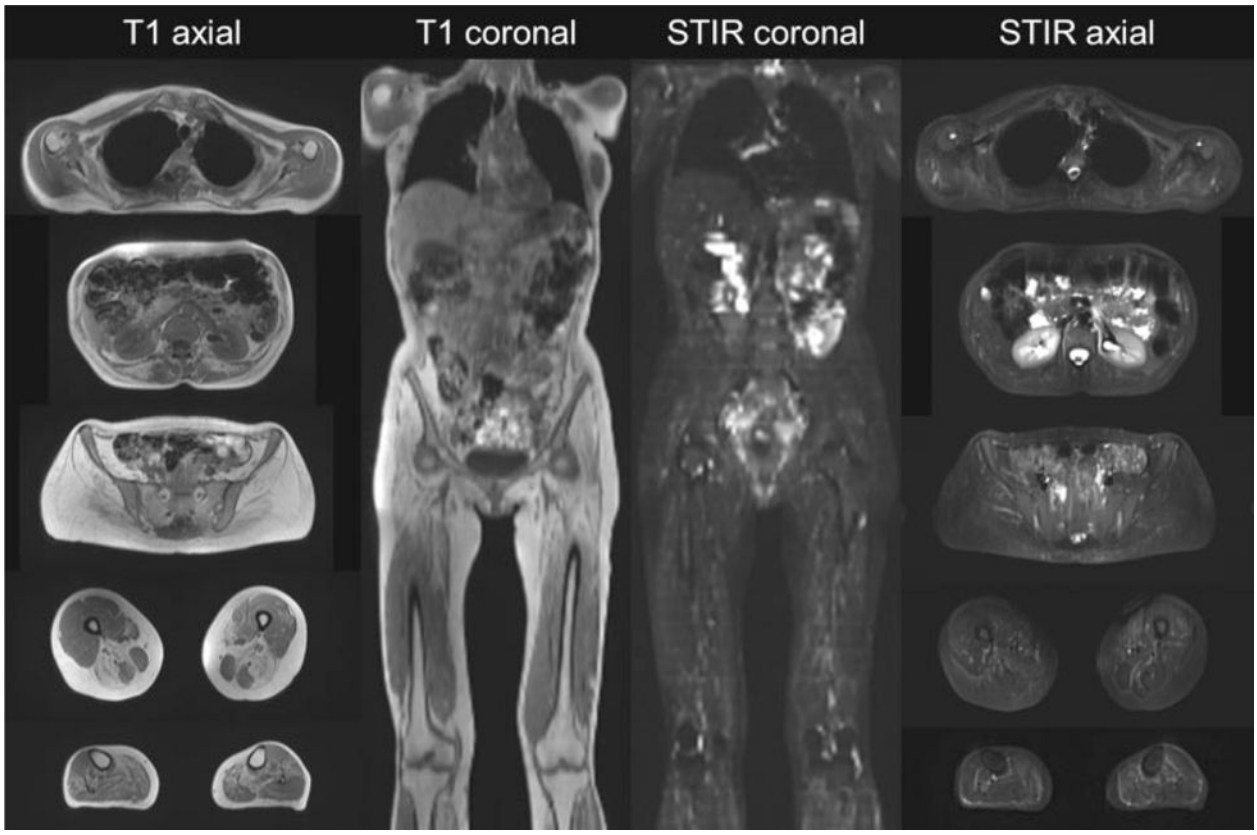

Fig. 3.
Representative examples of T1-weighted and short tau inversion recovery whole-body MR images in axial and coronal planes.

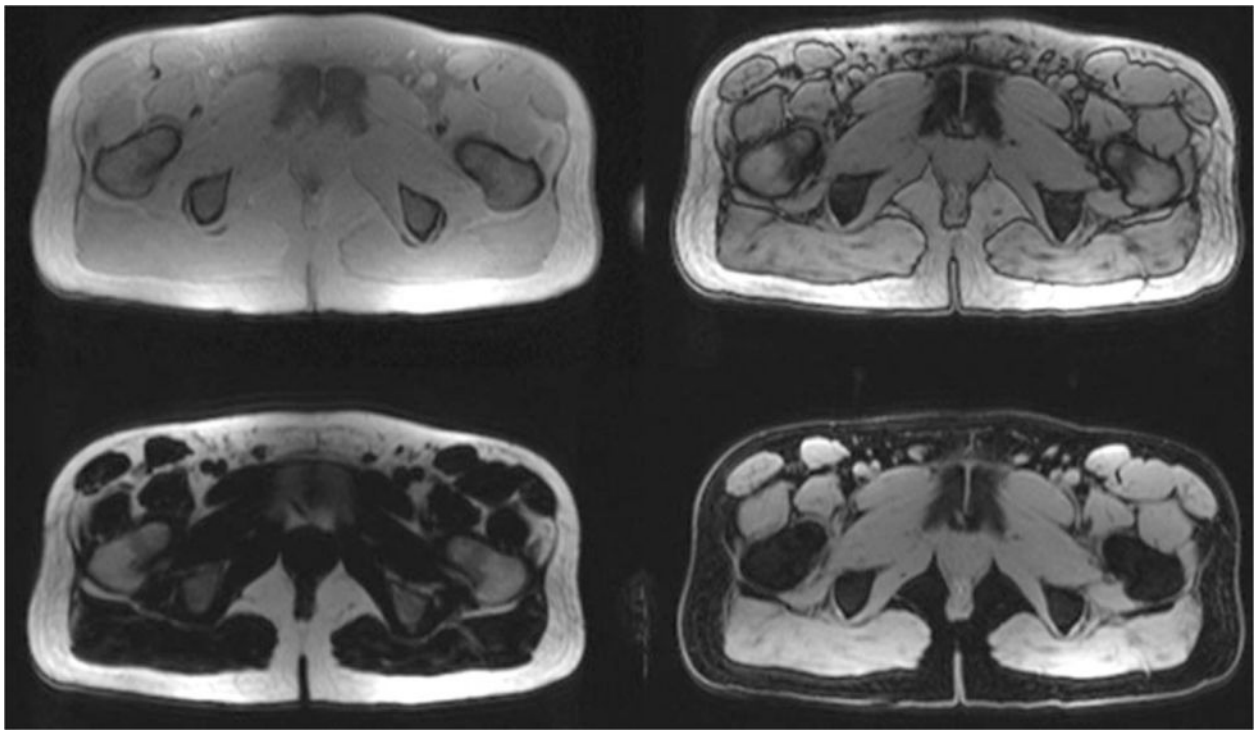

Fig. 4.

Representative axial cross sections of the upper leg of a healthy volunteer acquired using a 2-point Dixon sequence. The upper images are acquired with fat and water both in phase (left) and out of phase (right). The in- and out-of-phase images are used to construct the fat (left) and water (right) images in the lower row.

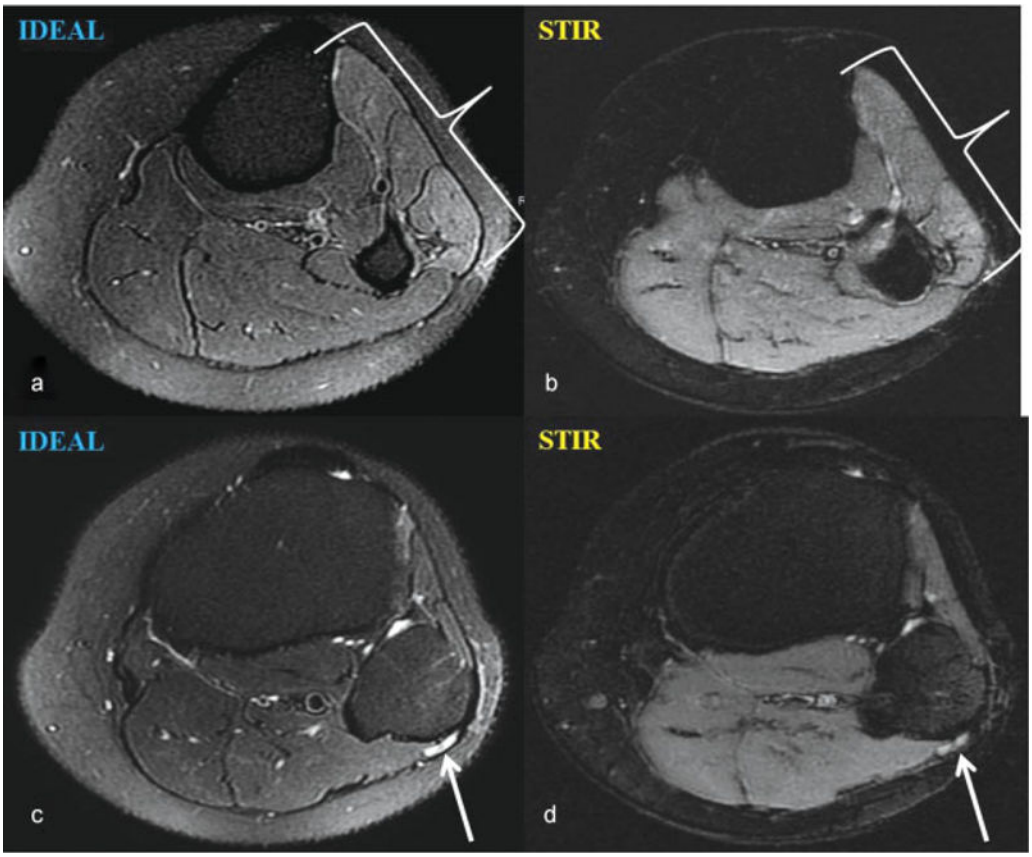

Fig. 5.

Axial T2-weighted iterative decomposition of water and fat with echo asymmetry and least-squares estimation (IDEAL) image performed on a 3.0-T magnet demonstrates (a) a denervation edema pattern within the anterior and lateral leg muscle compartments that cannot be confidently appreciated on the corresponding short tau inversion recovery (STIR) image (b). Signal hyperintensity of the common peroneal nerve as it courses around the fibular head is also more conspicuous on IDEAL (c) compared with STIR (d) imaging.

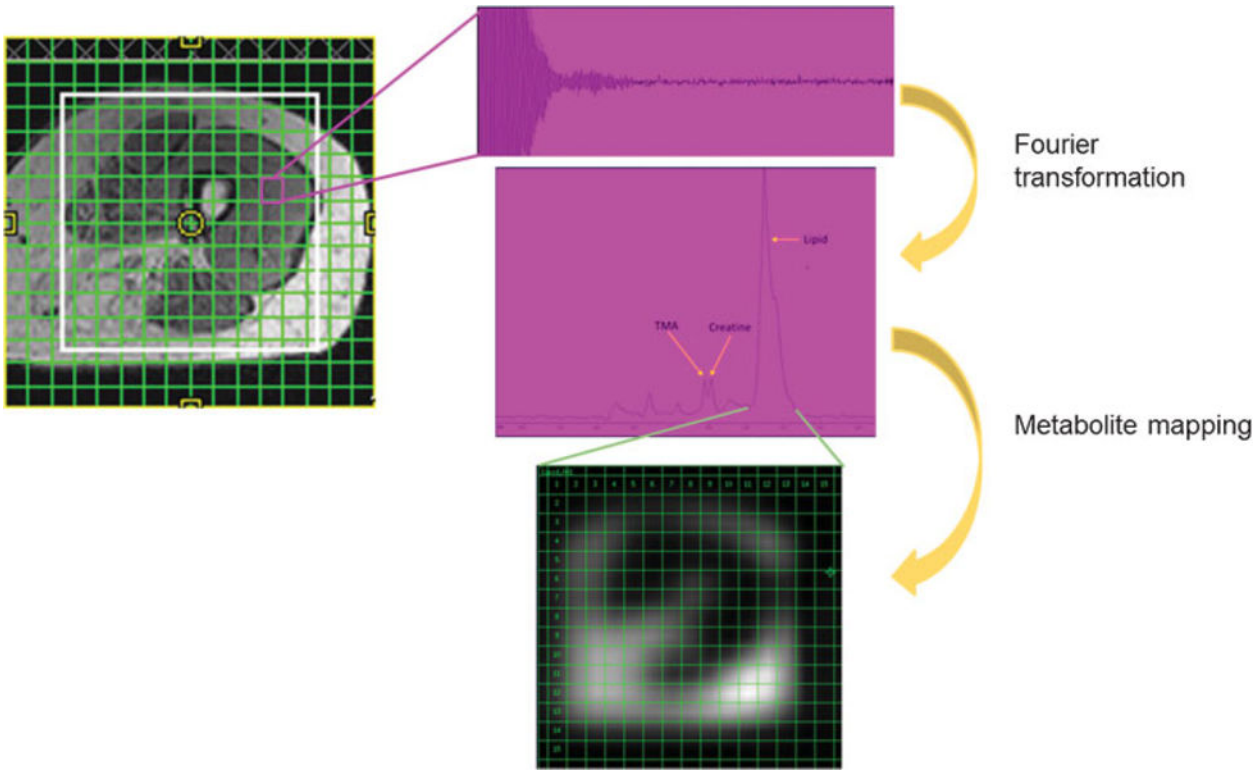

Fig. 6.

In multivoxel MR spectroscopy, a 16 × 16 grid is positioned over an axial T1 cross section of the midthigh of a patient with facioscapulohumeral muscular dystrophy. Extensive fatty infiltration is seen in the hamstrings. Spectra are generated from each voxel using Fourier transformation. Individual metabolite peaks (here, the lipid peak is selected) can be isolated from all of the voxels in the grid to generate metabolite maps.

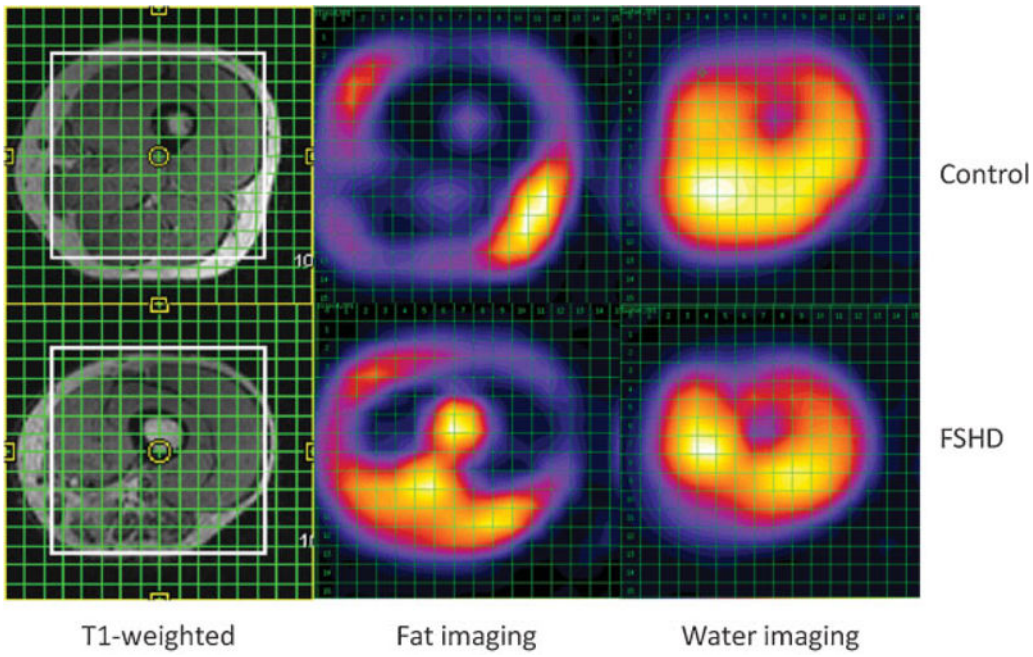

Fig. 7.

With multivoxel MR spectroscopy, 16 × 16 grids were placed over the midthigh of a healthy volunteer (top left) and a patient with facioscapulohumeral muscular dystrophy (FSHD) (bottom left). After Fourier transformation, corresponding spectra in the second and third columns show elevated fatty infiltration of the midthigh musculature in the FSHD patient, particularly in the posterior thigh in the region of the adductors and hamstrings. The control patient demonstrates a normal appearance and minimal degree of fatty infiltration of muscles of the midthigh.

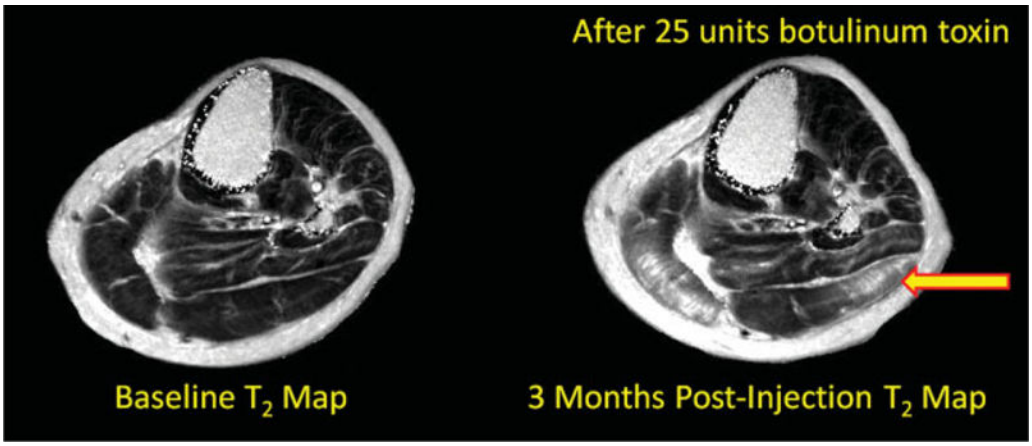

Fig. 8.

Axial T2 maps at baseline (left) and at 3 months after botulinum toxin injection (right) in a patient undergoing botulinum toxin injection for spasticity management. T2 mapping in this context is used to characterize botulinum toxin diffusion in human muscle using MRI. In the 3-month postinjection image, there are increased T2 values within the lateral head of the gastrocnemius muscle (yellow arrow).

Fig. 9.

Oblique sagittal (**a**) and coronal (**b**) T2-weighted Dixon fat suppression MR images demonstrate enlargement and signal hyperintensity (arrows) of the common peroneal nerve at the level of the fibular head. (**c**) There is subtly increased T2-weighted signal intensity of the tibialis anterior muscle (outlined) compared with normal regional muscles. (**d**) T2 maps of the same calf musculature, where region of interest (ROI) 1 exhibits a normal T2 value of the unaffected peroneal musculature (38.2 ± 1.5 ms) while ROI 2 demonstrates T2 prolongation of the anterior tibialis (49.8 ± 1.9 ms), confirming suspected denervation.

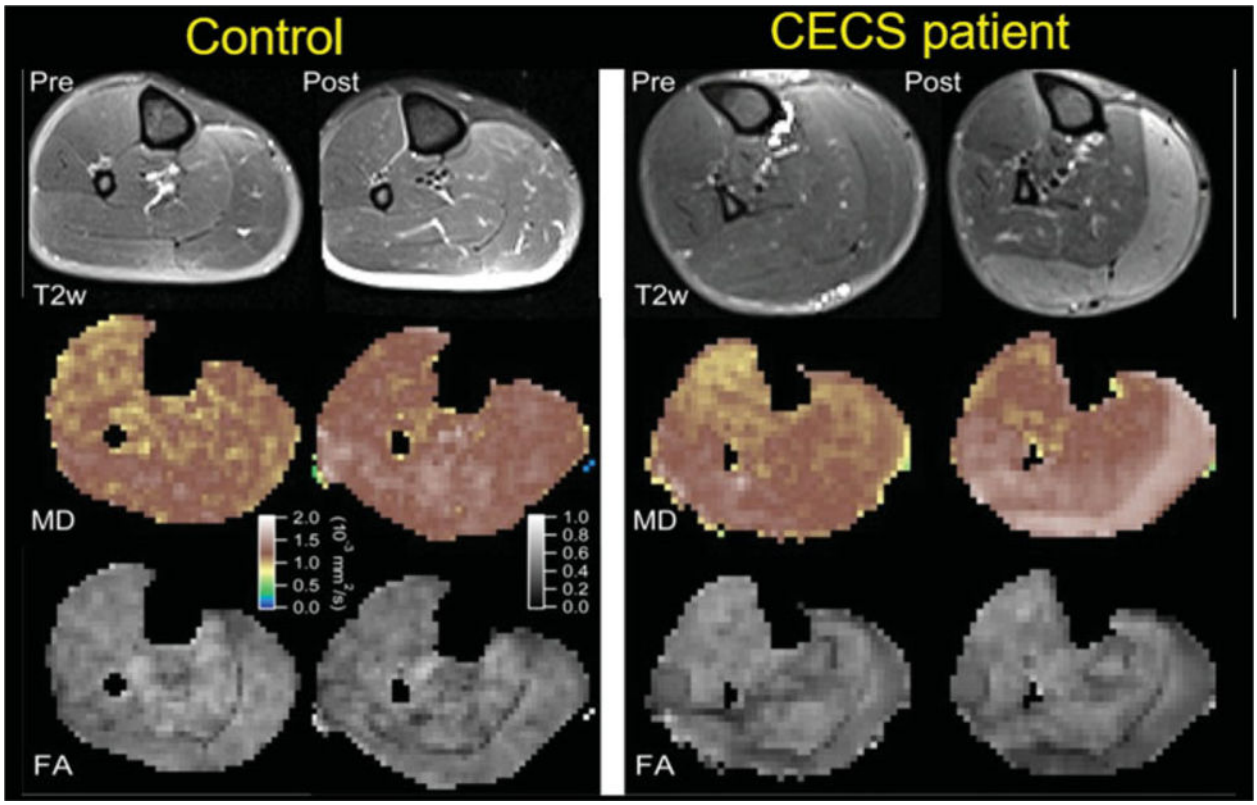

Fig. 10.

T2-weighted MRI and diffusion tensor imaging from a healthy volunteer (left) and a patient with chronic exertional compartment syndrome (CECS) (right) demonstrate right calf muscle before (labeled Pre) and after (labeled Post) treadmill exercise. In the CECS patient, there is clear increased T2 prolongation in the medial and lateral heads of the gastrocnemius that corresponds to areas of higher mean diffusivity (MD) and lower fractional anisotropy (FA). (Reprinted with permission from reference.[96])